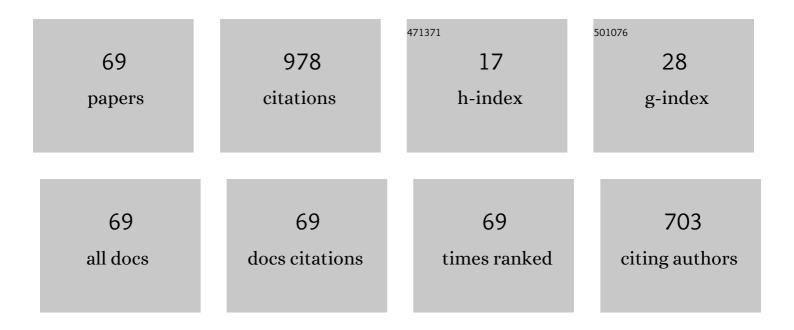
List of Publications by Year in descending order

Source: https://exaly.com/author-pdf/9193572/publications.pdf Version: 2024-02-01



SONCHE MENC

#	Article	IF	CITATIONS
1	Modeling nonlinear viscoelastic responses of flexible composites for soft robotics applications. Mechanics of Advanced Materials and Structures, 2023, 30, 2793-2805.	1.5	4
2	Intrinsic connections between thermionic emission cooling effect and emission characteristics of W-La2O3 cathodes at high temperatures. Materials Letters, 2022, 308, 131172.	1.3	5
3	Compressive experimental method and properties of C/C composites under ultra-high temperature environment. Journal of the European Ceramic Society, 2022, 42, 4702-4711.	2.8	9
4	The effect of fiber preform configuration on in-plane compressive behavior of high porosity needled carbon/carbon composites in elevated temperature environment. Ceramics International, 2022, 48, 25355-25367.	2.3	2
5	Crack-driving force and toughening mechanism in crustacean-inspired helicoidal structures. International Journal of Solids and Structures, 2021, 208-209, 107-118.	1.3	14
6	Oxyacetylene ablation resistance of continuous gradient ceramic–polymer composite. Corrosion Science, 2021, 179, 109050.	3.0	8
7	Analysis and simulation of fracture behavior in naturally occurring Bouligand structures. Acta Biomaterialia, 2021, 135, 473-482.	4.1	15
8	Quantification method for extrapolation errors of constitutive models and a demonstration on C/SiC composite. Composite Structures, 2021, 273, 114286.	3.1	1
9	Reconstruction of the heat transfer coefficient at the interface of a bi-material. Inverse Problems in Science and Engineering, 2020, 28, 374-401.	1.2	9
10	The use of cooled axial conduction guarded probe for the measurement of transient heat flux by calibrating the unit step response. International Journal of Heat and Mass Transfer, 2020, 147, 118850.	2.5	1
11	Growth of multi-morphology amorphous silicon oxycarbide nanowires during the laser ablation of polymer-derived silicon carbonitride. Ceramics International, 2020, 46, 2086-2092.	2.3	3
12	Global sensitivity analysis of low-velocity impact response of bio-inspired helicoidal laminates. International Journal of Mechanical Sciences, 2020, 187, 106110.	3.6	21
13	Effects of the liquid phase content on the microstructure and properties of the ZrW2O8 ceramics with negative thermal expansion fabricated by the cold sintering process. Journal of the European Ceramic Society, 2020, 40, 6079-6086.	2.8	12
14	Uncertainty Characterization Methods for Sparsely Sampled Quantity: A Tradeoff Analysis Considering Propagation. AIAA Journal, 2020, 58, 3129-3138.	1.5	0
15	An improved analytical method for calculating stiffness of 3D needled composites with different needle-punched processes. Composite Structures, 2020, 237, 111938.	3.1	15
16	Continuous gradient ceramic/polymer composite for application in large temperature gradient connection by a polymer-derived ceramic route. Composites Part A: Applied Science and Manufacturing, 2020, 132, 105799.	3.8	10
17	Perforation of needle-punched carbon-carbon composites during high-temperature and high-velocity ballistic impacts. Composite Structures, 2020, 245, 112224.	3.1	27
18	Impact and blast performance enhancement in bio-inspired helicoidal structures: A numerical study. Journal of the Mechanics and Physics of Solids, 2020, 142, 104025.	2.3	25

#	Article	IF	CITATIONS
19	Multi-fidelity uncertainty quantification method with application to nonlinear structural response analysis. Applied Mathematical Modelling, 2019, 75, 853-864.	2.2	6
20	Direct growth of flexible carbon nanotube interconnects during polymer-ceramic conversion reaction for release of thermal stress. Carbon, 2019, 153, 21-31.	5.4	3
21	Uncertainty quantification method for mechanical behavior of C/SiC composite and its experimental validation. Composite Structures, 2019, 230, 111516.	3.1	11
22	The stability and repeatability of high temperature electrical properties of SiAlCN ceramic sensor heads. Ceramics International, 2019, 45, 7588-7593.	2.3	19
23	Thermal stability and nanostructure evolution of amorphous SiCN ceramics during laser ablation in an argon atmosphere. Journal of the European Ceramic Society, 2019, 39, 4535-4544.	2.8	13
24	Modified double-notched specimen for ultra-high temperatures shear-strength testing of carbon/carbon composites. Journal of the European Ceramic Society, 2019, 39, 4654-4663.	2.8	11
25	Electrical conductivity change induced by porosity within polymer-derived SiCN ceramics. Journal of Alloys and Compounds, 2019, 777, 1010-1016.	2.8	20
26	Fabrication and Thermal Structural Characteristics of Ultra-high Temperature Ceramic Struts in Scramjets. Journal Wuhan University of Technology, Materials Science Edition, 2018, 33, 375-380.	0.4	4
27	A novel approach to temperature-dependent total emissivity estimation based on isothermal cooling. International Journal of Heat and Mass Transfer, 2018, 123, 122-128.	2.5	6
28	Experimental investigation on the mechanical behaviour of 3D carbon/carbon composites under biaxial compression. Composite Structures, 2018, 188, 7-14.	3.1	15
29	Continuous regulation from fully dense to high porosity within polymer-derived SiCN ceramics. Ceramics International, 2018, 44, 40-45.	2.3	6
30	Preparation and temperature-resistance characteristics of novel dense SiAlCN ceramics. Ceramics International, 2018, 44, 22473-22480.	2.3	12
31	improved laser ablation resistance of Si-C-N precursor derived ceramics in air. Ceramics International, 2018, 44, 23267-23272.	2.3	5
32	Development and validation of an anisotropic damage constitutive model for C/SiC composite. Ceramics International, 2018, 44, 22880-22889.	2.3	13
33	Experimental study of ultra-high temperature interlaminar tensile strengths of 3D-needled C/C composites using the V-shaped notched specimen compression method. Mechanics of Materials, 2018, 126, 26-35.	1.7	13
34	Electronic structures and optical properties of monoclinic ZrO2 studied by first-principles local density approximation + U approach. Journal of Advanced Ceramics, 2017, 6, 43-49.	8.9	66
35	Effective mitigation of the thermal short and expansion mismatch effects of an integrated thermal protection system through topology optimization. Composites Part B: Engineering, 2017, 118, 149-157.	5.9	18
36	Predicting the effective properties of 3D needled carbon/carbon composites by a hierarchical scheme with a fiber-based representative unit cell. Composite Structures, 2017, 172, 198-209.	3.1	28

#	Article	IF	CITATIONS
37	The damage-induced bi-modulus characteristic of C/SiC materials and experimental validation. Ceramics International, 2017, 43, 9171-9177.	2.3	10
38	Measurement of highâ€ŧemperature strains in superalloy and carbon/carbon composites using chemical composition gratings. Strain, 2017, 53, e12218.	1.4	1
39	Long-duration heat load measurement approach by novel apparatus design and highly efficient algorithm. Measurement Science and Technology, 2017, 28, 115901.	1.4	3
40	An inverse method for the estimation of a long-duration surface heat flux on a finite solid. International Journal of Heat and Mass Transfer, 2017, 106, 1087-1096.	2.5	13
41	ZrB2-CNTs Nanocomposites Fabricated by Spark Plasma Sintering. Materials, 2016, 9, 967.	1.3	13
42	Application of CCG Sensors to a High-Temperature Structure Subjected to Thermo-Mechanical Load. Sensors, 2016, 16, 1686.	2.1	1
43	Measurement of the high-temperature strain of UHTC materials using chemical composition gratings. Measurement Science and Technology, 2016, 27, 055101.	1.4	3
44	A novel method to evaluate the thermal shock behavior of ZrB2-SiC-graphite composites under alternating complex thermal stress environments. Ceramics International, 2016, 42, 16354-16358.	2.3	10
45	Investigation on Mechanical Properties of Porous Fiber Bundle-Matrix Interlayers in Three-Dimensional Carbon/Carbon Composite. Mechanics of Advanced Materials and Structures, 2014, 21, 810-815.	1.5	4
46	Optical properties of monoclinic HfO2 studied by first-principles local density approximation + U approach. Applied Physics Letters, 2013, 103, .	1.5	16
47	Real-time observation of damage nucleation in three-dimensionally reinforced carbon/carbon composites and role of bundle/matrix interface. Advanced Composite Materials, 2013, 22, 165-174.	1.0	3
48	Effect of environment atmosphere on thermal shock resistance of the ZrB2–SiC–graphite composite. Materials & Design, 2013, 50, 509-514.	5.1	26
49	The response of high-temperature optical fiber sensor applied to different materials. , 2013, , .		2
50	The connection technology based on high temperature silica fiber optic sensor. , 2012, , .		3
51	Repeated thermal shock behavior of the ZrB2–SiC–ZrC ultrahigh-temperature ceramic. Materials & Design, 2012, 35, 133-137.	5.1	26
52	A Homogenized Method Including Strain Gradients Based FFT Prediction of the Mechanical Properties of Composites. Polymers and Polymer Composites, 2011, 19, 367-376.	1.0	0
53	Radiative properties characterization of ZrB2–SiC-based ultrahigh temperature ceramic at high temperature. Materials & Design, 2011, 32, 377-381.	5.1	43
54	Mechanisms of material failure for fast heating up at the center of ultra high temperature ceramic. Solid State Sciences, 2010, 12, 527-531.	1.5	3

#	Article	IF	CITATIONS
55	Prediction of crack depth during quenching test for an ultra high temperature ceramic. Materials & Design, 2010, 31, 556-559.	5.1	13
56	Crack Patterns in Ceramic Plates after Quenching. Journal of the American Ceramic Society, 2010, 93, 3006-3008.	1.9	33
57	Experimental observation of ferromagnetism evolution in nanostructured semiconductor InN. Journal of Materials Chemistry, 2010, 20, 9935.	6.7	15
58	Real-Time Observation of Damage Nucleation in 3D Braided Carbon/Carbon Composites. Advanced Composites Letters, 2009, 18, 096369350901800.	1.3	1
59	The failure mechanism of ZrB2–SiC–graphite composite heated by high electric current. Materials Letters, 2009, 63, 2346-2348.	1.3	19
60	Effects of different additives on microstructure and crack resistance for an ultra-high temperature ceramic. International Journal of Refractory Metals and Hard Materials, 2009, 27, 813-816.	1.7	12
61	Valence electron structure of the (ZrTi)B2 solid solutions calculated by the three models. Science in China Series D: Earth Sciences, 2009, 52, 1195-1201.	0.9	4
62	Microstructure of a Mo-Si-C-N multi-layered anti-oxidation coating on carbon/carbon composites by fused slurry. Rare Metals, 2009, 28, 460-464.	3.6	1
63	Preparation and Thermal Ablation Behavior of HfB ₂ –SiCâ€Based Ultraâ€Highâ€Temperature Ceramics Under Severe Heat Conditions. International Journal of Applied Ceramic Technology, 2009, 6, 134-144.	1.1	24
64	Multiwalled Carbon Nanotubes–TiB ₂ –Ni Composite: Microstructure and Mechanical Properties. International Journal of Applied Ceramic Technology, 2009, 6, 525-530.	1.1	4
65	Mechanisms of thermal shock failure for ultra-high temperature ceramic. Materials & Design, 2009, 30, 2108-2112.	5.1	24
66	Magnetic properties of Mn-doped 6H-SiC. Applied Physics Letters, 2009, 94, .	1.5	58
67	Valence electron structure and properties of stabilized ZrO2. Science in China Series D: Earth Sciences, 2008, 51, 1008-1016.	0.9	1
68	Valence electron structure and properties of the ZrO2. Science in China Series D: Earth Sciences, 2008, 51, 1858-1866.	0.9	6
69	Oxidation behavior of zirconium diboride–silicon carbide at 1800°C. Scripta Materialia, 2007, 57, 825-828.	2.6	133